bioRxiv preprint doi: https://doi.org/10.1101/157099; this version posted September 21, 2018. The copyright holder for this preprint (which was not certified by peer review) is the author/funder, who has granted bioRxiv a license to display the preprint in perpetuity. It is made available under aCC-BY-NC-ND 4.0 International license.

Title:

Drug combinations targeting multiple cellular mechanisms enable axonal regeneration from crushed optic nerve into the brain

One Sentence Summary: Systems Biology approach to find novel drug combinations that can promote injured axons in the adult rat optic nerve to regenerate long distances.

Mustafa M. Siddiq[1], Yana Zorina[1], Arjun Singh Yadaw[1], Jens Hansen[1], Vera Rabinovich[1], Sarah M. Gregorich[2], Yuguang Xiong[1], Rosa E. Tolentino[1], Sari S. Hannila[3], Ehud Kaplan[1,4], Robert D. Blitzer[1], Marie T. Filbin[5]*, Christopher L. Passaglia[2] and Ravi Iyengar[1]

[1]Department of Pharmacological Sciences and Mount Sinai Institute for Systems Biomedicine, Icahn School of Medicine at Mount Sinai, New York , NY, 10029
[2]Departments of Chemical & Biomedical Engineering, 4202 E. Fowler Ave, ENB 118, University of South Florida Tampa, FL, 33620
[3]Department of Human Anatomy and Cell Science, Rm 130, Basic Medical Sciences Building, 745 Bannatyne Ave, Winnipeg, Manitoba R3E 0J9
[4]Department of Philosophy of Science, Charles University, Prague & the National Institute of Mental Health, Topolová 748, Klecany, Czechia
[5]Department of Biological Sciences, Hunter College, City University of New York NY, 10065
*Deceased January 15, 2014

Address correspondence to
Ravi Iyengar
Dept of Pharmacological Sciences, Box 1215
1425 Madison Rm 12-70
New York NY 10029
Ravi.iyengar@mssm.edu

bioRxiv preprint doi: https://doi.org/10.1101/157099; this version posted September 21, 2018. The copyright holder for this preprint (which was not certified by peer review) is the author/funder, who has granted bioRxiv a license to display the preprint in perpetuity. It is made available under aCC-BY-NC-ND 4.0 International license.

Abstract

Injured central nervous system axons do not regenerate, due to the limited intrinsic capacity of the neurons and the inhibitory environment at the injury site. Currently, there are no drugs or drug combinations to promote axonal regeneration in the injured spinal cord or optic nerve. We used a systems pharmacology approach to develop a four-drug combination, designed to regulate multiple subcellular processes at the cell body and the injured axon to promote regrowth of long projections through inhibitory environments. We tested this drug combination using the optic nerve crush model in rats. We intravitreally injected two drugs, HU-210 (cannabinoid receptor-1 agonist) and IL-6 (interleukin 6 receptor agonist) to stimulate retinal ganglion cell bodies (RGCs) whose axons had been crushed, and applied two other drugs in gel foam over the injury site: taxol to stabilize microtubules, and activated protein C (APC) to clear the injury site debris field. Dynamical computational models showed that the transcriptional effects of drugs applied at the cell body combined with drugs that work near the site of the injured axons could produce extensive synergistic growth by relief of inhibition at the growth cone. Morphology experiments show that the four-drug combination promotes axonal regeneration from the site of injury to the optic chiasm and the visual cortex. Electrophysiologically, the four-drug treatment restored pattern electroretinograms (pERG), and the animals had detectable visual evoked potentials (VEP) in the brain. We conclude that systems pharmacology-based drug treatment can promote functional axonal regeneration to the brain after nerve injury.

Introduction

Injury in the adult CNS is often permanent due to lack of ability of severed axons to regenerate. The inability to regenerate axons is attributed to two major causes: lack of intrinsic capacity of the CNS neurons in adult mammals to regenerate, and the presence of extracellular factors that inhibit axonal outgrowth (1-4). Myelin-associated molecules are thought to play a major role in inhibiting axonal regeneration (2, 5). In addition to this extrinsic inhibition, lack of appropriate activation of intracellular signaling pathways is also thought to play a role. Prominent among these are the MTOR (6) and STAT3 (7-8) pathways. Simultaneous inactivation of PTEN, an endogenous inhibitor of the MTOR pathway, and SOCS3, an endogenous inhibitor of the STAT3 pathway, led to robust and sustained axonal regeneration (9). Recently it was shown that sustained activation of the MTOR pathway by genetic manipulation, when combined with visual stimulation, leads to extended regeneration of optic nerve axons such that they reach the brain (10). Transcriptomic analyses of dorsal root ganglion (DRG) neurons following peripheral nerve injury have identified the potential involvement of numerous signaling pathways including neurotrophins, TGFβ cytokine, and JAK-STAT (11). Using these transcriptomic data and the Connectivity MAP, these researchers identified the drug ambroxol, a Na^+ channel inhibitor that promoted axon regeneration after optic nerve crush in mice (11). These observations suggest that

bioRxiv preprint doi: https://doi.org/10.1101/157099; this version posted September 21, 2018. The copyright holder for this preprint (which was not certified by peer review) is the author/funder, who has granted bioRxiv a license to display the preprint in perpetuity. It is made available under aCC-BY-NC-ND 4.0 International license.

drug therapy based on regulation of subcellular processes including cell signaling pathways could be a feasible approach to promote axon regeneration after nerve injury.

We have been studying signaling through the Go/i pathway for over two decades and found that activated Gαo activates STAT3 to promote oncogenic transformation (12). Studies of Neuro-2A cells treated with a cannabinoid receptor-1 (CB1R) agonist indicated that this receptor, acting through the GTPases Rap, Ral and Rac, activates Src and in turn STAT3 to stimulate neurite outgrowth (13-14). A more extensive study identified a complex upstream signaling network that controls STAT3 and CREB to regulate neurite outgrowth (15). These studies indicated that multiple receptors could regulate STAT3 to drive neurite outgrowth. IL-6 had been shown to promote neurite outgrowth in a PC-12 variant, and to overcome myelin-mediated inhibitors to promote neurite outgrowth in primary neurons (7, 16). We showed that submaximal, potentially therapeutic concentrations of the CB1R agonist HU-210 together with IL-6 could activate STAT3 in a sustained manner and induce neurite outgrowth in both Neuro2A cells and primary rat cortical neurons (17). Based on these observations we decided to test if a combination of these two drugs could promote axonal regeneration *in vivo* in the CNS in the rat optic nerve crush model.

In designing a potential combination therapy, we anticipated that stimulating signaling in the cell body of injured neurons alone probably would not lead to long-distance axon regeneration to the brain, and that we would need to modulate additional loci for extended axonal growth. Hence we sought to develop a systems-level combination therapy based on spatial specification of drug action. We identified drugs that could modulate subcellular function in the cell body and axon. We could then utilize this spatial information to develop a drug combination with the potential for treating CNS nerve injury by promoting long-range axonal regeneration. Since transcriptional regulation is critical for neurite outgrowth (15), we reasoned that CB1R and IL6R actions are likely to be in the cell body. We looked for subcellular processes in the axon that could be potential drug targets, and utilized computational dynamical models of neurite outgrowth (18) to predict how different subcellular processes could promote axonal regeneration. Based on these simulations we focused on microtubule growth, which is required for axon regeneration. Microtubules are stabilized by taxol, which has been shown to promote axonal regeneration (19). As axonal regeneration is inhibited by cell remnants at the site of injury, we hypothesized that such inhibition could be due to the incorporation of membrane vesicles at the growth cone (20). Treating the site of injury to potentially clear it of inhibitory agents and reduce the inflammatory response could also contribute to axonal regeneration. Based on these considerations, we chose a protease that could act locally to reduce the debris field and inhibit inflammation. We selected APC, which is a serine protease endogenous to the coagulation system (21) that is thought to be anti-inflammatory, and which promotes neuronal repair by stem cells in mice (22). In another study we independently observed that APC can promote limited axonal regeneration of crushed optic nerve in rat (23).

bioRxiv preprint doi: https://doi.org/10.1101/157099; this version posted September 21, 2018. The copyright holder for this preprint (which was not certified by peer review) is the author/funder, who has granted bioRxiv a license to display the preprint in perpetuity. It is made available under aCC-BY-NC-ND 4.0 International license.

The overall logic for this four-drug combination is schematically shown in Fig. 1. We decided to test if a combination of these drugs, two applied at the cell body and two at the axon at the site of injury, promoted long distance regeneration such that visual stimulation led to restoration of physiological function.

Results

Neurite outgrowth in microfluidic chambers with IL-6 and HU-210:

We previously found that submaximal concentrations of IL-6 and HU-210 in combination have an additive effect on neurite outgrowth for rat cortical neurons in primary culture (17). We tested if this effect could be observed for regeneration of growing neurites that had been severed *in vitro*. For these experiments we used microfluidic chambers, where the cell bodies could be compartmentalized from the growing axons (Fig. 2Aa). We plated primary rat cortical neurons on a permissive substrate in these chambers, and allowed them to grow long neurites. To mimic axotomy, we lesioned all the neurites in the chambers on the right side and then added HU-210 and IL-6 to one side or the other (Fig. 2Ab). Application of IL-6 and HU-210 to the cell bodies (somal; left side of chamber) significantly promoted neurite growth up to 300 µm from the soma; in contrast, drug application to the axonal compartment was less effective, and offered no benefit when add to somal drug application (Fig. 2A, c-d). We then repeated the experiment using myelin, a non-permissive substrate (Fig. 2B). We observed that addition of IL-6 and HU-210 to the cell bodies promoted longer growth of axotomized processes in the presence of myelin, compared to either treatment alone.

We also examined the effects of IL-6 and HU-210 on neurite outgrowth in cortical neurons. When whole myelin was used as the substrate, IL-6 and HU-210 promoted neurite outgrowth, overcoming the inhibitory effect of myelin (Figs. 2C&D and Supplementary Fig. 1). As previously reported in Neuro2A cells (17), the combination of IL-6 and HU-210 in cortical neurons stimulated STAT3 by phosphorylation at Tyr705 (Fig. 2E, and Supplementary Fig. 1), consistent with our earlier observation that HU-210-stimulated neurite outgrowth depends on Stat3-mediated transcription (17). We confirmed the presence of the receptors for IL-6 (gp130) and CB1(CB1R) in our cortical cultures by RT-PCR, as shown in Supplementary Fig. 2I. We also detected the receptors by immunolabeling, and found both gp130 and CB1R were expressed in the somal compartment of microfluidic chambers (Supplementary Fig. 2II). The combination of IL-6 and HU-210 did not significantly enhance neuronal survival after axotomy (Supplementary Fig. 2III).

Drug Treatment for Axonal Regeneration *in vivo*

To test whether treatment with HU-210 and IL-6 promotes axon regeneration following injury in vivo, we used the optic nerve crush (ONC) model in Fisher rats (24). Following surgery, we treated the injured eye with HU-210 and IL-6 injected intravitreally, and after two weeks we evaluated for regeneration, first by sectioning the nerve and immunostaining with GAP-43

bioRxiv preprint doi: https://doi.org/10.1101/157099; this version posted September 21, 2018. The copyright holder for this preprint (which was not certified by peer review) is the author/funder, who has granted bioRxiv a license to display the preprint in perpetuity. It is made available under aCC-BY-NC-ND 4.0 International license.

antibody (Figs. 3A&B). We observed a promoting effect of combined HU-210 and IL-6 treatment, the majority of the crushed axons without drug treatment had no detectable GAP-43 labeling even 0.2mm distal to the crush site, while intravitreal injections of a combination of HU-210 + IL-6 resulted in detectable axons nearly 3mm away from the crush site (Fig. 3B). In additional studies we visualized regenerating processes by labeling the axons with cholera toxin-B subunit (CTB) coupled to Alexa-488 (25), chemically clearing the nerves using the 3-DISCO technique (26), and obtaining maximum intensity projection images (Figs. 3C&D). The 3-DISCO technique allowed us to image the crush site from proximal to distal end, and to examine the Z-stack to confirm that the crush was complete with no spared fibers. To evaluate the efficiency of the crush method, we performed ONC with no drug treatment and CTB-labeled the nerves immediately afterwards. When we examined the nerve 3 days later, we observed complete crushes in the brightfield setting and the CTB-label was not detected past the crush site (Fig, 2F). Moreover, we examined each nerve for evidence of any spared fibers; an example is shown in Supplementary Fig. 3A. Samples with such incomplete crushes were excluded from further analysis. In nerves from animals that received intravitreal injections of IL-6 & HU-210, we could observe CTB-labeled fibers over 2 mm from the crush site (Figs. 3D&D'). Fluorescence was quantified at 250-µm intervals from the crush site, revealing a striking difference between the treated and untreated groups (Fig. 3E).

The effectiveness of HU-210 and IL-6 in the ONC model was confirmed in Long-Evans rats. Axonal regeneration was not observed in animals that received either no drug treatment or treatment with submaximal doses of intravitreally injected IL-6 or HU-210 individually, as assessed by CTB-labeled fibers 0.2 mm distal to the crush site (Fig. 4A-C). In contrast, the combination of intravitreal IL-6 and HU-210 resulted in significant axon growth, extending on average more than 0.5 mm beyond the crush site (Fig. 2D). While the effect of HU-210 + IL-6 was less pronounced than that observed in Fisher rats, subsequent experiments were restricted to Long-Evans rats because the albino phenotype of Fisher rats makes them unsuitable for retinal electrophysiology.

Our overall goal was to devise a drug therapy that would provide sufficient regeneration after the optic nerve crush so that we could restore communication between the eye and the brain. The observations here and our previous biochemical data (15, 17) indicate that the effects of HU-210 and IL-6, injected intravitreally, likely reflect upregulated biosynthetic processes. To promote more robust growth we decided to additionally apply drugs that could work at the injury site. We looked for additional subcellular processes that could be targeted by drugs. For this we utilized a dynamical model of neurite outgrowth that we have recently developed (18) that is focused on understanding how activities of groups of subcellular processes are balanced to produce a whole-cell response. In this computational model we had studied how microtubule growth and membrane vesicle transport and fusion at the growth cones are together responsible for neurite growth. These simulations indicated that simultaneously regulating microtubule

bioRxiv preprint doi: https://doi.org/10.1101/157099; this version posted September 21, 2018. The copyright holder for this preprint (which was not certified by peer review) is the author/funder, who has granted bioRxiv a license to display the preprint in perpetuity. It is made available under aCC-BY-NC-ND 4.0 International license.

dynamics and membrane vesicle dynamics could greatly enhance axon regeneration. Taxol is known to stabilize dynamic microtubules, leading to elongation of stable microtubules, and thus promotes axonal regeneration (19). To enhance membrane vesicle delivery-related subcellular processes, we focused on external inhibitors of axonal growth, including myelin-associated proteins such as Nogo. Biochemical experiments have shown that Nogo receptors and gangliosides mediate glycoprotein inhibition of neurite outgrowth (27) and binding of extracellular agents such as Nogo to gangliosides can promote endocytosis (28), thus disrupting membrane delivery to the growth cone plasma membrane which is essential for continued growth of the axon. Since the site of injury contains many such myelin-related proteins, to relieve inhibition we decided to test the application of a protease that could act locally. For this we chose APC (activated protein C), which has been reported to promote neuronal repair (22). We used gel foam to apply taxol or APC to the site of injury, either alone or in combination with HU-210 and IL-6 applied at the cell body through intravitreal injection. Taxol alone in gelfoam had a modest effect on promoting some regenerating fibers as reported earlier (Fig. 4E) (29). APC alone promoted significant axonal regeneration about 0.5 mm past the crush site (Fig. 4G). The effect of APC was most prominent on one edge of the nerve, presumably where we had placed the drug-impregnated gelfoam (Fig. 4G). In order to ascertain whether these were spared fibers, we carefully examined the crush site of this nerve treated with APC (Supplementary Fig. 3C) and observed that the crush was in fact complete, with regenerating CTB-labeled fibers growing along the edge of the nerve. Combining IL-6 and HU-210 with taxol gelfoam (Fig 4F) produced a more robust response compared to the three agents individually or IL-6 and HU-210 combined, growing over 0.5 mm distal to the crush site. However, none of the drugs tested could promote extensive axonal regeneration individually. More extensive growth was observed when APC was combined with IL-6 and HU-210 (Fig 4H).

A 4-drug combination promotes optic nerve regeneration to the chiasm

We then tested a four-drug combination with intravitreal injection of HU-210 and IL-6 to deliver these agents to the retinal ganglion cell body, and application of taxol and APC in gelfoam at the site of injury. We sacrificed the animals after 3 weeks of drug treatment. Three days prior to euthanasia we intravitreally injected CTB in some animals to visualize the regenerated axons. The whole nerve was chemically cleared using the 3-DISCO technique (26). In other animals, nerve sections were immunostained for GAP-43. We observed that 7 out 29 animals tested (5 with CTB-labeling and 2 with GAP-43 immunostaining) had regenerating axons that could be detected at the chiasm, a distance of 7.5 mm from the crush site (Fig 5-IA,B) Another four animals with the four-drug treatment combination showed modest axonal regeneration extending about 3 mm from the crush site (Table 1A). Quantification of the extent of CTB label for each condition tested is provided in Fig 5-IB. In Supplementary Fig. 4A, we include magnified images of the crush site (SFig. 4A) from Fig. 5-IAb' that had 4-drug treatment and highlighted sections demarcated by the asterisk (SFig. 4A'& A") displaying the crush is complete as there are no spared fibers growing along the edge. Fig. 5-I and Supplementary Fig. 4 are maximum intensity

bioRxiv preprint doi: https://doi.org/10.1101/157099; this version posted September 21, 2018. The copyright holder for this preprint (which was not certified by peer review) is the author/funder, who has granted bioRxiv a license to display the preprint in perpetuity. It is made available under aCC-BY-NC-ND 4.0 International license.

projections using the 3-DISCO method of clearing, which are 2-D flattened generated images of approximately 540 Z-slices. We looked at individual slices within the same nerve (slice #240 and #274 out of 537, Supplementary Fig 5A&B) and found CTB-labeled fibers growing in torturous pattern from the crush and even 1mm away from the crush site, as highlighted in the closeups.

A number of additional experiments are shown in the Supplementary Figs. 4&5 to establish that what we observe are regenerated fibers. In Supplementary Fig. 3A, we show an example of an incomplete crush. With the 3-DISCO technology we could examine all the CTB-labeled axons in the nerve bundle, and we can observed spared fibers toward the bottom edge demarcated by an arrow. When we observed such a sample, the animal was disqualified from the study. In Supplementary Fig. 3B shows an uninjured nerve with CTB labeling, illustrating the full extent of fibers with the optic nerve bundle. We also waited 7days post CTB labeling (Fig. 5-II) we detected robust axonal regeneration from the crush site (Fig. 5-IIB) into the chiasm (Fig. 5-IIC). A close up view of the crush site is provided in Supplementary Fig 6A, with inverted image colors to show that our crushes are complete with no observable sparing. In the chiasm, we saw torturous growth of regenerating axons with CTB label as they grow into the chiasm from the injured side (Fig. 5-IIC') and to the opposing side (Figs. 5-IIC" & C'"). In this particular animal we sectioned the contralateral brain and observed with immunostaining for CTB that there was label in superior colliculus, an area innervated by the optic nerve (Fig. 5-IID and close-up of the image in Fig. 5-III).

In separate studies, using the iDISCO technique we labeled the whole nerve with antibodies against GAP-43 and then chemically cleared them (see Supplementary Fig. 7) (30). Both CTB-labeled and GAP43-immunostained chemically cleared nerves were imaged using a multiphoton microscope. Supplementary Fig. 7 shows, the crush site where GAP-43 axons regenerated past the crush site (top panel), in close proximity to the chiasm (middle panel) the closeup box shows GAP-43+ staining (Supplementary Fig. 7B'). The bottom panel we have GAP-43-labeled axons detected in the chiasm, as demarcated by the asterisks and in the closeup boxes (Supplementary Figs. 7C' and C'). All of these experiments provide additional support that the CTB-labeled nerves observed in Fig. 5-I are regenerated axons.

Dynamical computational models indicate that relief of inhibition could be a mechanism underlying the extensive axonal regeneration.

To gain insight into the mechanism by which the four-drug combination promotes extensive regeneration, we modeled the effects of these drugs on neuronal growth processes. We used the top-down version of a neurite-outgrowth multicompartment ODE model that we developed previously (18). This model analyzes the dynamics of a whole-cell process in terms of interactions between three subcellular processes: *Production of Membrane Components, Vesicle Transport and Exocytosis*, *and Microtubule Growth.* This model is based on the microtubule growth model developed by Margolin et al. (31) and the vesicle transport model of Heinrich and

bioRxiv preprint doi: https://doi.org/10.1101/157099; this version posted September 21, 2018. The copyright holder for this preprint (which was not certified by peer review) is the author/funder, who has granted bioRxiv a license to display the preprint in perpetuity. It is made available under aCC-BY-NC-ND 4.0 International license.

Rapaport (32). Our simulations show that the highly synergistic effects of the four drugs on axon growth can be quantitatively explained by assuming that a transcription-mediated increase in the biosynthesis of components required for axonal growth (by HU-210 and IL-6) such that molecular components needed for axonal growth are not limiting, combined with stabilization of growing microtubules by by taxol and removal of inhibitory extracellular factors by APC can suppress vesicle fusion at the growth cone. Relief of inhibition of vesicle fusion by APC greatly enhances the ability of the other three drugs to drive axonal regeneration resulting in apparent synergy. Key results from the computational modeling are shown in Supplementary Figures 11-13. Details of the computational models are provided in the Supplementary Material (*Computational Model of Drug Effects on Neurite Outgrowth*).

The 4-drug combination treatment partially restores electroretinograms and cortical visual evoked potential in animals subjected to optic nerve crush

We tested if the morphologically observed axonal regeneration led to restoration of functional electrophysiological responses. Pattern electroretinograms (pERG) were recorded from both eyes of rats with one crushed optic nerve to determine if the four-drug combination could improve overall retinal electrophysiology, particularly of RGCs (33) (Fig. 6A). In normal non-injured eyes, pERGs elicited by a full-field contrast-reversing grating are characterized by a small initial negative component approximately 35 ms after pattern reversal (N35), followed by a larger positive component between 45-60 ms (P50), and finally a large negative component at 90-100 ms (N95). However, the injured eye of control animals with only vehicle injections had an aberrant pERG, while injured animals that received the four-drug combination treatment showed partial pERG recovery in the injured eye. The recovery approached pre-injury responses for the P50 component. These observations indicate that the four-drug combination stabilizes the cell bodies of the injured retinal ganglion neurons leading to some recovery of electrophysiological function.

pERGs reflect the physiology of retinal neuronal cell bodies, but not of optic nerve axons themselves (33). Since we obtained some degree of axonal regeneration into the brain with the four-drug treatment, we asked whether there is concomitant recovery of brain electrophysiological responses to visual stimuli. We stimulated each eye with a series of light flashes at different intensities (0.001 to 100% of maximum) and simultaneously recorded the flash ERG (fERG), which is indicative of activity in all neuronal cells of the retina (not just the RGC that innervates the optic nerve), and the visual evoked potential (VEP) detected bilaterally from the primary visual cortex. Figure 6B-D shows representative fERGs for light flashes to the uninjured eye (Figure 6B), the injured eye of a vehicle-treated animal (Figure 6C), and the injured eye of a drug-treated animal (Figure 6D). fERG signals were reduced at all intensities for injured with vehicle treatment relative to the uninjured control side, consistent with neurodegeneration that occurs due to the crush. The fERGs in animals that received the four-drug treatment appeared nearly normal, indicating that the therapy was neuroprotective for injured retinal neurons. In Figure 6E, we show the VEP for flashes to the non-injured eye. The

bioRxiv preprint doi: https://doi.org/10.1101/157099; this version posted September 21, 2018. The copyright holder for this preprint (which was not certified by peer review) is the author/funder, who has granted bioRxiv a license to display the preprint in perpetuity. It is made available under aCC-BY-NC-ND 4.0 International license.

VEP is slow and monotonic at lower intensities (<0.1%) and becomes markedly faster and multiphasic at higher intensities. The VEP is absent for flashes to the injured eye of vehicle-treated animals (Fig. 6F). In contrast, VEPs were detected at high light intensities in a subset of animals that were treated with the four-drug combination (Fig. 6G). The signal was slow and monotonic in these animals, similar to non-injured eyes at low light intensities. We performed statistical analysis on the VEP records by comparing them to traces recorded after weak flashes that yielded no apparent VEP, and setting a threshold for detectability (see Methods). We found that responses for all of the vehicle-treated animals (n = 7) were not significantly different from noise, even at the highest flash intensities. However, 5 of 19 drug-treated animals showed VEP responses above the cut-off criterion at some flash intensity (Fig 6H and Table1B), indicating partial restoration of functional connectivity in those animals. Data of VEP recordings for three individual animals for the non-injured eye, injured with vehicle only (no treatment), and injured with four-drug treatment are shown in Supplementary Figs. 8-10.

Discussion

In this study, we designed a drug therapy for a complex pathophysiology by using systems-based logic. We considered the multiple subcellular processes occurring at different locations within the cell that could be involved in axonal regeneration, and identified drugs that could regulate these subcellular processes. We focused on drugs that would increase capacity for regeneration at the neuronal cell body, and enhance the ability of the axons to grow longer by modulating local subcellular processes in the axonal shaft. We made the assumption that the process of neurite outgrowth in vitro involves many if not all of the subcellular processes that neurons use regenerate axons in vivo. Cell signaling experiments in our laboratory had shown that transcriptional regulation through STAT3 and CREB played a major role in neurite outgrowth (12, 17). Independent studies had shown a role for the cAMP pathway (2) and SOCS3, a STAT inhibitor (9). Hence we reasoned that application of receptor ligands that stimulate the STAT3 pathway among other transcriptional regulators (15) could increase the intrinsic capacity of neurons to regenerate. Since CB-1 and IL-6 receptors are expressed in adult neurons, we selected agonists for these receptors as regenerative drugs. In vitro experiments showed that application of these drugs at the cell body was more effective in promoting regeneration, and hence in vivo we applied the drug at the cell body as well. As we used the optic nerve crush model, we injected the receptor agonists intravitreally so that they could act on the RGC cell bodies. This resulted in modest but significant drug-stimulated axon regeneration beyond the site of injury. These experiments provided us with an important guideline: that not only should we select the right subcellular process to target, but also that the drug should be applied at the right location. Using this reasoning we selected the two core sets of subcellular processes that function within the growing axon and could targeted by drugs: microtubule growth, and membrane expansion at the growth cone. Since taxol stabilizes dynamic microtubules, thus allowing axonal processes to grow, we applied taxol to the growing axonal regions. By integrating observations in the literature (27, 28), we reasoned that the debris at the injury site including myelin-associated

bioRxiv preprint doi: https://doi.org/10.1101/157099; this version posted September 21, 2018. The copyright holder for this preprint (which was not certified by peer review) is the author/funder, who has granted bioRxiv a license to display the preprint in perpetuity. It is made available under aCC-BY-NC-ND 4.0 International license.

proteins might inhibit axonal growth by inhibiting the exocytotic delivery of membranes to the growth cone, which is needed for axonal growth. Hence, we selected a locally acting protease that could clear the debris field and block these inhibitory agents. Our experiments show that this combination of increasing capacity at the cell body and modulating subcellular processes in the growing axon enables substantial regeneration from the site of injury to the visual cortex, such that we were able to partially restore electrophysiological communication from the eye to the visual cortex. Our results provide an example of the systems therapeutic approach providing a rational basis for the design of therapies to treat complex pathophysiologies, in this case nerve damage in the CNS.

Although it is encouraging that we have an identifiable path for a systems logic-based design of rational therapeutics, much further work is needed to translate these findings into viable treatments even in animal models. We have not considered dosing regimens or adverse events associated with this drug therapy. We also need to establish the relationship between the extent of recovery of electrophysiological function and vision-dependent behaviors in the whole animal. These types of experiments will form the basis for future studies. Nevertheless, since observations in the optic nerve crush model are most often applied to spinal cord injury, it will be useful to test if this four-drug combination can reverse spinal cord injury and restore some movement.

bioRxiv preprint doi: https://doi.org/10.1101/157099; this version posted September 21, 2018. The copyright holder for this preprint (which was not certified by peer review) is the author/funder, who has granted bioRxiv a license to display the preprint in perpetuity. It is made available under aCC-BY-NC-ND 4.0 International license.

Literature Cited

1. He Z. and Jin Y. Intrinsic Control of Axon Regeneration. *Neuron* **90**, 437-51 (2016).
2. Filbin M.T. Myelin-associated inhibitors of axonal regeneration in the adult mammalian CNS. *Nat. Rev. Neurosci*. **4**, 703-13 (2004).
3. Cajal R.Y. (1991). Cajal's Degeneration & Regeneration of the Nervous System. Oxford Press.
4. Galtrey C.M. and Fawcett, J.W. The role of chondroitin sulfate proteoglycans in regeneration and plasticity in the central nervous system. *Brain Res. Rev*. **54**, 1-18 (2007).
5. Buchli A. D. and Schwab M.E. Inhibition of Nogo: a key strategy to increase regeneration, plasticity and functional recovery of the lesioned central nervous system. *Ann. Med*. **37**, 556-67 (2005).
6. Park KK, Liu K, Hu Y, Smith PD, Wang C, Cai B, Xu B, Connolly L, Kramvis I, Sahin M and He Z. Promoting axon regeneration in the adult CNS by modulation of the PTEN/mTOR pathway. *Science*. **322**,963-966 (2008).
7. Wu YY and Bradshaw RA. Induction of Neurite Outgrowth by Interleukin-6 Is Accompanied by Activation of Stat3 Signaling Pathway in a Variant PC12 Cell (E2) Line. *J. Biol. Chem*. **271**, 13023-13032 (1996).
8. Quarta S, Baeumer BE, Scherbakov N, Andratsch M, Rose-John S, Dechant G, Bandtlow CE and Kress M. Peripheral Nerve Regeneration and NGF-Dependent Neurite Outgrowth of Adult Sensory Nerurons Converge on STAT3 Phosphorylation Downstream of Neuropoietic Cytokine Receptor gp130. *J Neurosci*. **34**, 13222-13233 (2014).

bioRxiv preprint doi: https://doi.org/10.1101/157099; this version posted September 21, 2018. The copyright holder for this preprint (which was not certified by peer review) is the author/funder, who has granted bioRxiv a license to display the preprint in perpetuity. It is made available under aCC-BY-NC-ND 4.0 International license.

9. Sun F, Park KK, Belin S, Wang D, Lu T, Chen G, Zhang K, Yeung C, Feng G, Yankner BA and He Z. Sustained axon regeneration induced by co-deletion of PTEN and SOCS3. *Nature*. **480**,372-375 (2011).

10. Bei F, Lee HHC, Liu X, Gunner G, Jin H, Ma L, Wang C, Hou I, Hensch TK, Frank E, Sanes JR, Chen C, Fagiolini M and He Z. Restoration of Visual Function by Enhancing Conduction in Regenerated Axons. *Cell*. **164**, 219-232 (2016).

11. Chandran V, Coppola G, Nawabi H, Omura T, Versano R, Huebner EA, Zhang A, Costigan M, Yekkirala A, Barrett L, Blesch A, Michaelevski I, Davis-Turak J, Gao F, Langfelder P, Horvath S, He Z, Benowitz L, Fainzilber M, Tuszynski M, Woolf CJ and Geschwind DH. A Systems-Level Analysis of the Peripheral Nerve Intrinsic Axonal Growth Program. *Neuron*. **89**, 956-970 (2016).

12. Ram PT, Horvath CM, Iyengar R. Stat3-mediated transformation of NIH-3T3 cells by constitutively active Q2505L Gαo protein. *Science* **287**, 142-4 (2000).

13. Jordan J.D., He J.C., Eungdamrong N.J., Gomes I., Ali W., Nguyeng T., Bivona T.G., Philips M.R., Devi L.A. and Iyengar R. Cannabinoid receptor-induced neurite outgrowth is mediated by Rap1 activation through G(alpha)o/i-triggered proteasomal degradation of Rap1GAPII. *J. Biol. Chem*. **280**, 11413-21 (2005).

14. He J.C., Gomes I., Nguyeng T., Jayaram G., Ram P.T., Devi L.A. and Iyengar R. The G alpha(o/i)-coupled cannabinoid receptor-mediated neurite outgrowth involves Rap regulation of Src and Stat3. *J. Biol. Chem*. **280**, 33426-34 (2005).

15. Bromberg K.D., Maayan A., Neves S.R. and Iyengar R. Design Logic of a cannabinoid receptor signaling network that triggers neurite outgrowth. *Science* **320**, 903-9 (2008).

bioRxiv preprint doi: https://doi.org/10.1101/157099; this version posted September 21, 2018. The copyright holder for this preprint (which was not certified by peer review) is the author/funder, who has granted bioRxiv a license to display the preprint in perpetuity. It is made available under aCC-BY-NC-ND 4.0 International license.

16. Cao Z, Gao Y, Bryson JB, Hou J, Chaudhry N, Siddiq M, Martinez J, Spencer T, Carmel J, Hart RP and Filbin MT. The Cytokine Interleukin-6 Is Sufficient But Not Necessary to Mimic the Peripheral Conditioning Lesion Effect on Axonal Growth. *J. Neurosci*. **26**,5565-5573 (2006).

17. Zorina Y., Iyengar R. and Bromberg K.D. Cannabinoid 1 receptor and interleukin-6 receptor together induce integration of protein kinase and transcription factor signaling to trigger neurite outgrowth. *J. Biol. Chem*. **285**, 1358-70 (2010).

18. Yadaw A., Siddiq M., Rabinovich V., Iyengar R. and Hansen J. Dynamic balance between vesicle transport and microtubule growth enables neurite growth. bioRxiv doi: https://doi.org/10.1101/153569. (2017).

19. Hellal F., Hurtado A., Ruschel J., Flynn K.C., Laskowski C.J., Umlauf M., Kapitein L.C., Strikis D., Lemmon V., Bixby J., Hoogenraad C.C. and Bradke F. Microtubule stabilization reduces scarring and causes axon regeneration after spinal cord injury. *Science* **331**, 928-931 (2011).

20. Koseki H, Donegá M, Lam BYH, Petrova V, van Erp S, Yeo GSH, Kwok JCF, ffrench-Constant C et al. Selective rab11 transport and the intrinsic regenerative ability of CNS axons. *eLife* **6**:e26956 (2017).

21. Mosnier L.O., Zlokovic B.V. and Griffin J.H. The cytoprotective protein C pathway. *Blood*. **109**,3161-3172 (2007).

22. Wang Y., Zhao Z., Rege S.V., Wang M., Si G., Zhou Y., Wang S., Griffin J.H., Goldman S.A. and Zlokovic B.V. 3K3A-activated protein C stimulates postischemic neuronal repair by human neural stem cells in mice. *Nature Med*. **22**. 1050-55 (2016).

bioRxiv preprint doi: https://doi.org/10.1101/157099; this version posted September 21, 2018. The copyright holder for this preprint (which was not certified by peer review) is the author/funder, who has granted bioRxiv a license to display the preprint in perpetuity. It is made available under aCC-BY-NC-ND 4.0 International license.

23. Siddiq M.M., Hannila S.S., Zorina Y., Nikulina E., Rabinovich V., Hou J., Huq R., Richman E.L., et al. Activated Protein C blocks the inhibitory effect on neurite outgrowth by extracellular histones that mediates its inhibition through a retrograde YB-1 signal. bioRxiv doi: https://doi.org/10.1101/365825 (2018).

24. Leon S., Yin Y., Nguyen J., Irwin N. and Benowitz L.I. Lens injury stimulates axon regeneration in the mature rat optic nerve. *J. Neurosci*. **20**, 4615-4626 (2000).

25. Siddiq M.M., Hannila S.S., Carmel J.B., Bryson J.B., Hou J., Nikulina E., Willis M.R., Mellado W., Richman E.L., Hilaire M., Hart R.P. and Filbin M.T. Metallothionein-I/II Promotes Axonal Regeneration in the Central Nervous System. *J. Biol. Chem*. **290**, 16343-16356 (2015).

26. Ertürk A., Mauch C.P., Hellal F., Förstner F., Keck T., Becker K., Jährling N., Steffens H., Richter M., Hübener M., et al. Three-dimensional imaging of the unsectioned adult spinal cord to assess axon regeneration and glial responses after injury. *Nat. Med*. **18**, 166-171 (2012).

27. Mehta N.R., Lopez P.H., Vyas A.A. and Schnaar R.L. Gangliosides and Nogo receptors independently mediate myelin-associated glycoprotein inhibition of neurite outgrowth in different nerve cells. *J. Biol. Chem*. **282**, 27875-86 (2007).

28. Fewou S.N., Plomp J.J. and Willison H.J. The pre-synaptic motor nerve terminal as a site for antibody-mediated neurotoxicity in autoimmune neuropathies and synaptopathies. *J Anat*. **224**, 36-44 (2014).

29. Sengottuvel V., Leibinger M., Pfreimer M. and Fischer D. Taxol facilitates axon regeneration in the mature CNS. *J. Neurosci*. **16**, 2688-99 (2011).

bioRxiv preprint doi: https://doi.org/10.1101/157099; this version posted September 21, 2018. The copyright holder for this preprint (which was not certified by peer review) is the author/funder, who has granted bioRxiv a license to display the preprint in perpetuity. It is made available under aCC-BY-NC-ND 4.0 International license.

30. Renier N., Wu Z., Simon D.J., Yang J., Ariel P. and Tessier-Lavigne M. iDISCO: A Simple, Rapid Method to Immunolabel Large Tissue Samples for Volume Imaging. *Cell* **159**, 896-910 (2014).

31. Margolin, G., Gregoretti, I.V., Cickovski, T.M., Li, C., Shi, W., Alber, M.S., and Goodson, H.V. The mechanisms of microtubule catastrophe and rescue: implications from analysis of a dimer-scale computational model. *Molecular biology of the cell* ***23***, 642-656 (2012).

32. Heinrich, R., and Rapoport, T.A. Generation of nonidentical compartments in vesicular transport systems. *The Journal of cell biology* **168**, 271-280 (2005).

33. Fiorentini A., Maffei L., Pirchio M., Spinelli D. and Porciatti V. The ERG in response to alternating gratings in patients with diseases of the peripheral visual pathway. *Invest. Opthalmol. Vis. Sci.* **21**, 490-3 (1981).

34. Mukhopadhyay G., Doherty P., Walsh F.S., Crocker P.R. and Filbin M.T. A novel role for myelin-associated glycoprotein as an inhibitor of axonal regeneration. *Neuron* **13**, 757-67 (1994).

35. Husain S., Abdul Y. and Crosson C.E. Preservation of Retinal Ganglion Cell Function by Morphine in a Chronic Ocular-Hypertensive Rat Model. *Invest. Opthalmol. Vis. Sci.* **53**, 4289-98 (2012).

36. Tang X., Tzekov R. and Passaglia C.L. Retinal cross talk in the mammalian visual system. *J. Neurophysiol*. **115**, 3018-29 (2016).

bioRxiv preprint doi: https://doi.org/10.1101/157099; this version posted September 21, 2018. The copyright holder for this preprint (which was not certified by peer review) is the author/funder, who has granted bioRxiv a license to display the preprint in perpetuity. It is made available under aCC-BY-NC-ND 4.0 International license.

37. Dixit R., Ross J.L., Goldman Y.E. and Holzbaur, E.L. Differential regulation of dynein and kinesin motor proteins by tau. *Science* **319**, 1086-1089 (2008).

38. Ebneth A., Godemann R., Stamer K., Illenberger S., Trinczek B. and Mandelkow E. Overexpression of tau protein inhibits kinesin-dependent trafficking of vesicles, mitochondria and endoplasmic reticulum: implications for Alzheimer's disease. *The Journal of cell biology* **143**, 777-794 (1998).

39. Hagiwara H., Yorifuji H., Sato-Yoshitake R. and Hirokawa N. Competition between motor molecules (kinesin and cytoplasmic dynein) and fibrous microtubule-associated protiens in binding to microtubules. *J. Biol. Chem* **269**, 3581-3589 (1994).

40. LaPointe N.E., Morfini G., Pigino G., Gaisina I.N., Kozikowski A.P., Binder L.I. and Brady S.T. The amino terminus of tau inhibits kinesin-dependent axonal transport: implications for filament toxicity. *Journal of neuroscience research* **87**, 440-451 (2009).

41. Seitz A. , Kojima H., Oiwa K., Mandelkow E.M., Song Y.H. and Mandelkow E. Single-molecule investigation of the interference between kinesin, tau amd MAP2c. The *EMBO Journal* **21**, 4896-4905 (2002).

42. Vershinin M., Carter B. C., Razafsky D.S., King S.J. and Gross S.P. Multiple-motor based transport and its regulation by Tau. *Proceedings of the National Academy of Sciences of the United States of America* **104**, 87-92 (2007).

43. Desai A and Mitchison TJ. Microtubule polymerization dynamics. *Annu Rev Cell Dev Biol* **13**, 83-117 (1997).

44. Fadic, R., Vergara, J., and Alvarez, J. Microtubules and caliber of central and peripheral processes of sensory axons. *J Comp Neurol* **236**, 258-264 (1985).

bioRxiv preprint doi: https://doi.org/10.1101/157099; this version posted September 21, 2018. The copyright holder for this preprint (which was not certified by peer review) is the author/funder, who has granted bioRxiv a license to display the preprint in perpetuity. It is made available under aCC-BY-NC-ND 4.0 International license.

45. Harris, K.M., and Stevens, J.K. Dendritic spines of CA 1 pyramidal cells in the rat hippocampus: serial electron microscopy with reference to their biophysical characteristics. *J Neurosci.* **9**, 2982-2997 (1989).

46. Beller, J.A., Kulengowski, B., Kobraei, E.M., Curinga, G., Calulot, C.M., Bahrami, A., Hering, T.M., and Snow, D.M. Comparison of sensory neuron growth cone and filopodial responses to structurally diverse aggrecan variants, in vitro. *Exp. Neurol.* **247**, 143-157 (2013).

47. Vale, R.D., Funatsu, T., Pierce, D.W., Romberg, L., Harada, Y., and Yanagida, T. Direct observation of single kinesin molecules moving along microtubules. *Nature* **380**, 451-453 (1996).

48. Carter, N.J., and Cross, R.A. Mechanics of the kinesin step. *Nature* **435**, 308-312 (2005).

49. King, S.J., and Schroer, T.A. Dynactin increases the processivity of the cytoplasmic dynein motor. *Nat. Cell Biol.* **2**, 20-24 (2000).

50. Nishiura, M., Kon, T., Shiroguchi, K., Ohkura, R., Shima, T., Toyoshima, Y.Y., and Sutoh, K. A single-headed recombinant fragment of Dictyostelium cytoplasmic dynein can drive the robust sliding of microtubules. *J Biol. Chem.* **279**, 22799-22802 (2004).

51. Zhang, B., Koh, Y.H., Beckstead, R.B., Budnik, V., Ganetzky, B., and Bellen, H.J. Synaptic vesicle size and number are regulated by a clathrin adaptor protein required for endocytosis. *Neuron* **21**, 14651475 (1998).

52. Kunda, P., Paglini, G., Quiroga, S., Kosik, K., and Caceres, A. Evidence for the involvement of Tiam1 in axon formation. *J Neurosci.* **21**, 2361-2372. (2001).

bioRxiv preprint doi: https://doi.org/10.1101/157099; this version posted September 21, 2018. The copyright holder for this preprint (which was not certified by peer review) is the author/funder, who has granted bioRxiv a license to display the preprint in perpetuity. It is made available under aCC-BY-NC-ND 4.0 International license.

Table 1A: Summary of Optic Nerve Regeneration in Long Evans Rats.

Treatment	Number of Animals tested	Regenerating axons not detected past crush site	Regenerating axons at least 3 mm from crush site	Regenerating axons to the chiasm (nearly 8 mm from crush site)
No treatment	11	11	0	0
4-Drug Combination	29	18	4	7

Table 1B: Summary of Visual Evoked Potentials (VEP)

Treatment	Number of Animals tested	Number of Animals with VEP in response to light
No treatment	7	0
4-Drug Combination	19	5

Note Tables 1A and B are two separate groups of animals.

bioRxiv preprint doi: https://doi.org/10.1101/157099; this version posted September 21, 2018. The copyright holder for this preprint (which was not certified by peer review) is the author/funder, who has granted bioRxiv a license to display the preprint in perpetuity. It is made available under aCC-BY-NC-ND 4.0 International license.

Acknowledgements:

This research was supported by Supported by NIH grants R01GM54508 and Systems Biology Center grant P50GM071558. Multiphoton microscopy was performed in the Microscopy CORE at the Icahn School of Medicine at Mount Sinai and was supported with funding from NIH Shared Instrumentation Grant 1S10RR026639-01. The authors declare no competing financial interests.

Author contributions:

M.M.S., Y.Z., M.T.F. and R.I. developed the overall concept for this project. Y.Z., M.M.S., V.R. and R.E.T. performed all in vitro experiments. M.M.S., V.R. and R.E.T. performed all surgical procedures. M.M.S. performed all chemical clearing and imaging on Olympus Multiphoton Microscope and Zeiss LSM 880 Microscope. M.M.S. and S.S.H. performed all image analysis. J.H., A.S.Y. and R.I. developed and executed the Dynamical computational models. E.K., C.L.P., M.M.S. and R.I. designed the in vivo electrophysiological experiments. M.M.S., V.R., S.M.G. and C.L.P. performed and analyzed all data for the in vivo electrophysiology. Y.X. and R.D.B. helped analyze in vivo electrophysiological recordings and performed Z-score analysis. M.M.S., R.D.B. and R.I. wrote the manuscript. All co-authors critically reviewed and edited the manuscript.

Figure 1

Spatial Systems Reasoning for Combinational Therapy to promote CNS axonal regeneration

Figure 1A

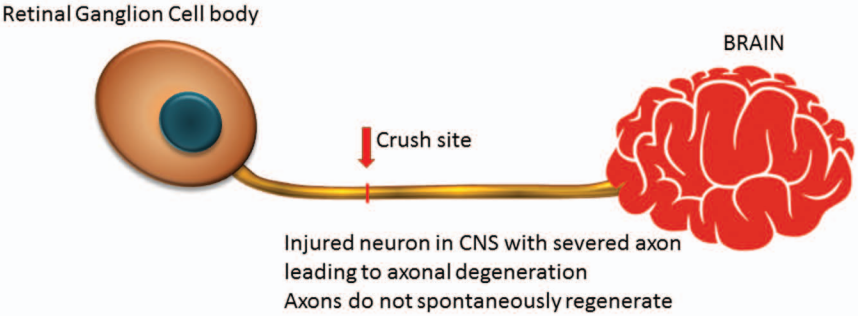

Figure 1B

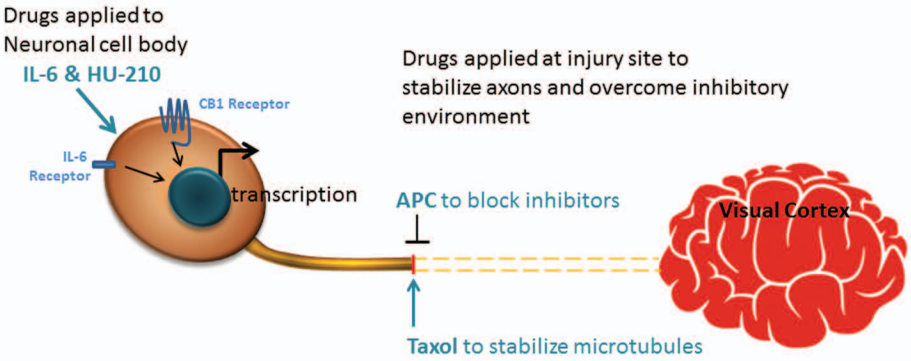

bioRxiv preprint doi: https://doi.org/10.1101/157099; this version posted September 21, 2018. The copyright holder for this preprint (which was not certified by peer review) is the author/funder, who has granted bioRxiv a license to display the preprint in perpetuity. It is made available under aCC-BY-NC-ND 4.0 International license.

Figure1: Spatial Systems Reasoning for Combinational Therapy to promote CNS axonal regeneration. A. Diagrammatic cartoon of a neuron displaying the retinal ganglion cell body whose axon is crushed leading to axonal degeneration and severing connection to the brain. The axon will degenerate from crush site. B. Our four-drug combination delivery is to apply drugs to both the neuronal cell bodies and to the injury site. Two drugs injected intravitreally to the cell body – IL-6 and HU-210, which will bind to their respective receptors – IL-6R and CB1R, that will elicit a downstream signal to the nucleus to initiate transcription. Another two drugs will be administered in gelfoam to the injury site, where APC will contribute to overcome inhibitors in the injured environment and Taxol to stabilize injured microtubules.

Figure 2

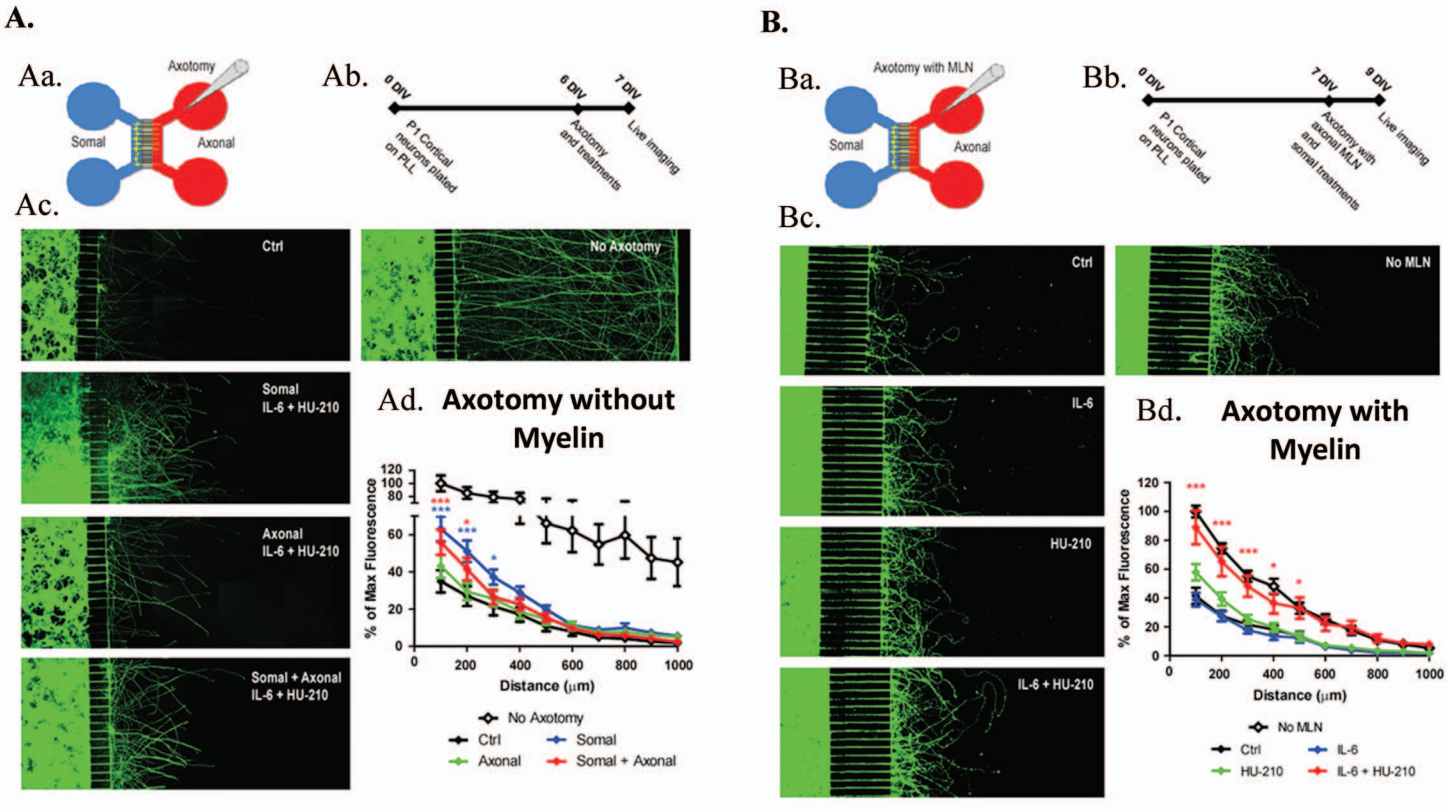
A.
Aa.
Axotomy
Somal
Axonal
Ab.
0 DIV
6 DIV
7 DIV
P1 Cortical neurons plated on PLL
Axotomy and treatments
Live imaging
Ac.
Ctrl
No Axotomy
Somal IL-6 + HU-210
Axonal IL-6 + HU-210
Somal + Axonal IL-6 + HU-210
Ad. Axotomy without Myelin
% of Max Fluorescence
Distance (μm)
No Axotomy
Ctrl
Somal
Axonal
Somal + Axonal
B.
Ba.
Axotomy with MLN
Somal
Axonal
Bb.
0 DIV
7 DIV
9 DIV
P1 Cortical neurons plated on PLL
Axotomy with axonal MLN and somal treatments
Live imaging
Bc.
Ctrl
No MLN
IL-6
HU-210
IL-6 + HU-210
Bd. Axotomy with Myelin
% of Max Fluorescence
Distance (μm)
No MLN
Ctrl
IL-6
HU-210
IL-6 + HU-210

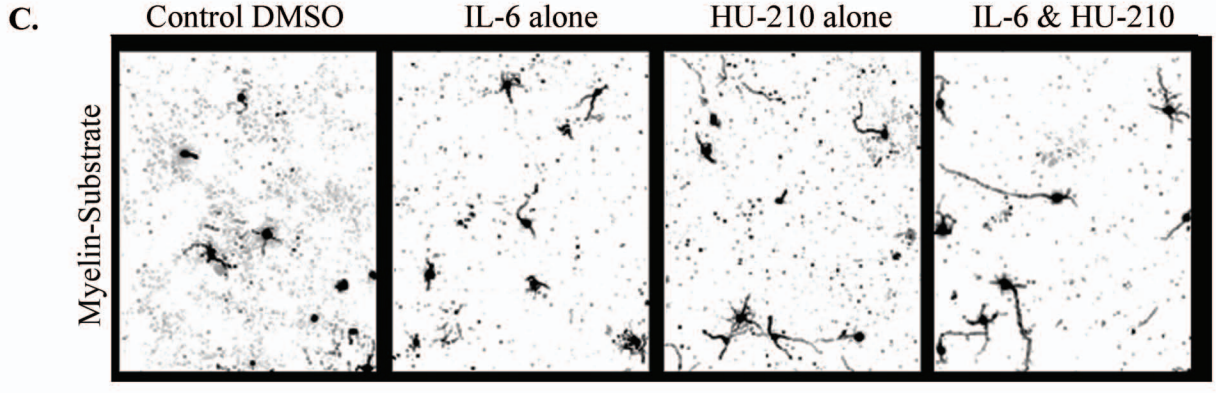
C.
Control DMSO
IL-6 alone
HU-210 alone
IL-6 & HU-210
Myelin-Substrate

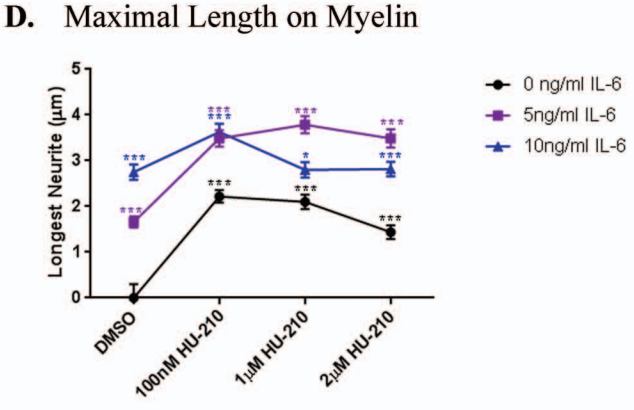
D. Maximal Length on Myelin
Longest Neurite (μm)
0 ng/ml IL-6
5ng/ml IL-6
10ng/ml IL-6
DMSO
100nM HU-210
1μM HU-210
2μM HU-210

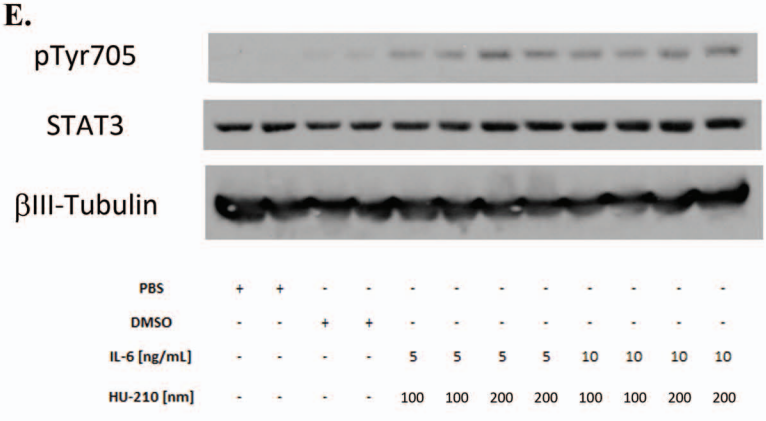
E.
pTyr705
STAT3
βIII-Tubulin
PBS + + - - - - - - - - - -
DMSO - - + + - - - - - - - -
IL-6 [ng/mL] - - - - 5 5 5 5 10 10 10 10
HU-210 [nm] - - - - 100 100 200 200 100 100 200 200

bioRxiv preprint doi: https://doi.org/10.1101/157099; this version posted September 21, 2018. The copyright holder for this preprint (which was not certified by peer review) is the author/funder, who has granted bioRxiv a license to display the preprint in perpetuity. It is made available under aCC-BY-NC-ND 4.0 International license.

Figure 2A. Somal application of IL-6 and HU-210 results in enhanced neurite outgrowth after axotomy. Cortical neurons were plated in the somal compartment (blue) of microfluidic chambers, schematically represented in (Aa.) and allowed to grow axons across the microgrooves into the axonal compartment (red). The gray cone depicts a pipet used to perform axotomy by aspirating medium from the axonal compartment. (Ab.) For axotomy experiments, neurons were cultured in chambers on PLL for 6-7 days, and axotomy was performed by aspirating all medium from the axonal compartments 2-4 times. 5 ng/ml IL-6 and 100 nM HU-210 were added together to the somal, axonal or both compartments after axotomy. Treatments were added to the indicated compartments in neurobasal (NB) immediately after axotomy, and neurons were imaged live after 24 hrs using Calcein AM. (Ac.) Representative confocal images after axotomy and treatment. (Ad.) Neurite outgrowth was quantified by measuring the total fluorescence at multiple cross-sections of the image. The zero point on the x-axis represents the right edge of microgrooves. All data points were normalized to the first point of "No Axotomy" at 100 μm from the microgrooves as 100 percent. Statistical differences were calculated from two independent experiments using two-way ANOVA. Asterisks show significance compared to Ctrl treatment at a given distance; *, $p < 0.05$; ***, $p < 0.001$.

Figure 2B. Somal treatment with IL-6 and HU-210 promotes neurite outgrowth on myelin (MLN). (Ba.) Schematic representation of the microfluidic chamber. (Bb.) Neurons were cultured in chambers on PLL for 7 days, and axotomy was performed. The axonal compartment was then filled with 20 μg/ml solution of myelin (MLN) in NBS. IL-6/HU-210 treatments were applied to the somal compartment of each respective chamber. The neurons were imaged live after 48 hrs using Calcein AM. (Bc.) Representative confocal images of neurons following axotomy and treatment. (Bd.) Neurite outgrowth was quantified by measuring the total fluorescence at multiple cross-sections of the image. The zero point on the x-axis represents the right edge of microgrooves. All data points were normalized to the first point of "No MLN" as 100 percent. Statistical differences were calculated from four independent experiments using two-way ANOVA. Asterisks show significance compared to Ctrl treatment at a given distance; *, $p < 0.05$; ***, $p < 0.001$.

Figures 2C & D. Stimulation of cortical neurons with IL-6 and HU-210 together promotes neurite outgrowth on myelin in a dose-dependent manner. P1 cortical neurons were plated on myelin–coated slides and treated with IL-6 and/or HU-210 over a range of concentrations. The neurons were fixed after 24 hrs and labeled for β-III-tubulin. Quantifications of neurite outgrowth were performed from 1500-2000 cells per condition. The bar graphs show mean ± S.E.M. of the longest neurite of each cell on myelin. Statistical differences were calculated using a one-way ANOVA followed by Bonferroni's multiple comparison test. Black asterisks show significance between the treatment and DMSO alone; blue or purple asterisks show significance between each combinational treatment and the sole HU-210 treatment at the corresponding concentration; *, $p<0.05$; ***, $p<0.001$. Fig. 1-IV. Representative images of neurons plated on myelin (MLN) substrate treated from top to bottom, with either DMSO, IL-6, HU-210 or IL-6&HU-210 labeled with β-III-tubulin.

bioRxiv preprint doi: https://doi.org/10.1101/157099; this version posted September 21, 2018. The copyright holder for this preprint (which was not certified by peer review) is the author/funder, who has granted bioRxiv a license to display the preprint in perpetuity. It is made available under aCC-BY-NC-ND 4.0 International license.

Figure 2E. Combination of IL-6 and HU-210 activates STAT-3. Cortical neurons in non-supplemented neurobasal media were treated with IL-6 and HU-210 or DMSO for controls for 2hours. The cells were lysed and subjected to immunoblot analysis for phospho-STAT3 (p-Tyr705), total STAT3 and βIII-tubulin. We normalized the samples for phospho-STAT3 to total STAT3 and made a bar graph with the fold changes.

bioRxiv preprint doi: https://doi.org/10.1101/157099; this version posted September 21, 2018. The copyright holder for this preprint (which was not certified by peer review) is the author/funder, who has granted bioRxiv a license to display the preprint in perpetuity. It is made available under aCC-BY-NC-ND 4.0 International license.

Figure 3

A.

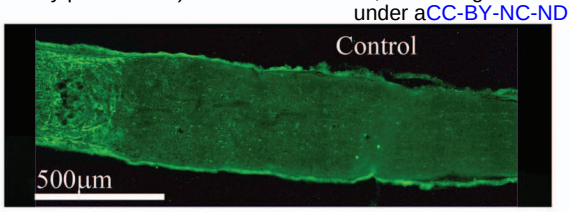

GAP-43 immunostaining in sectioned slices

B.

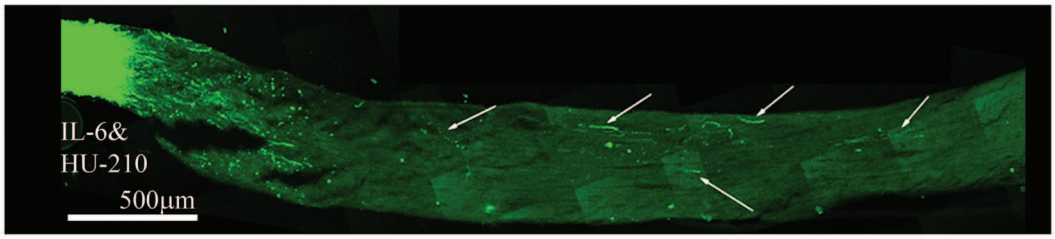

3-DISCO Clearing and Full nerve imaging of CTB-labeled axons

C.

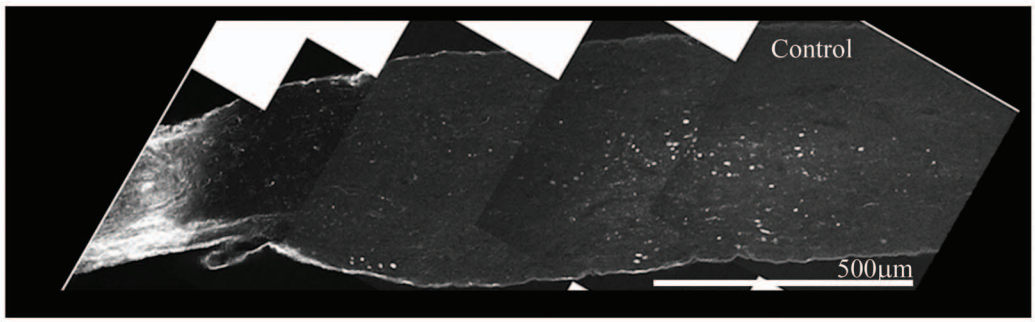

D.

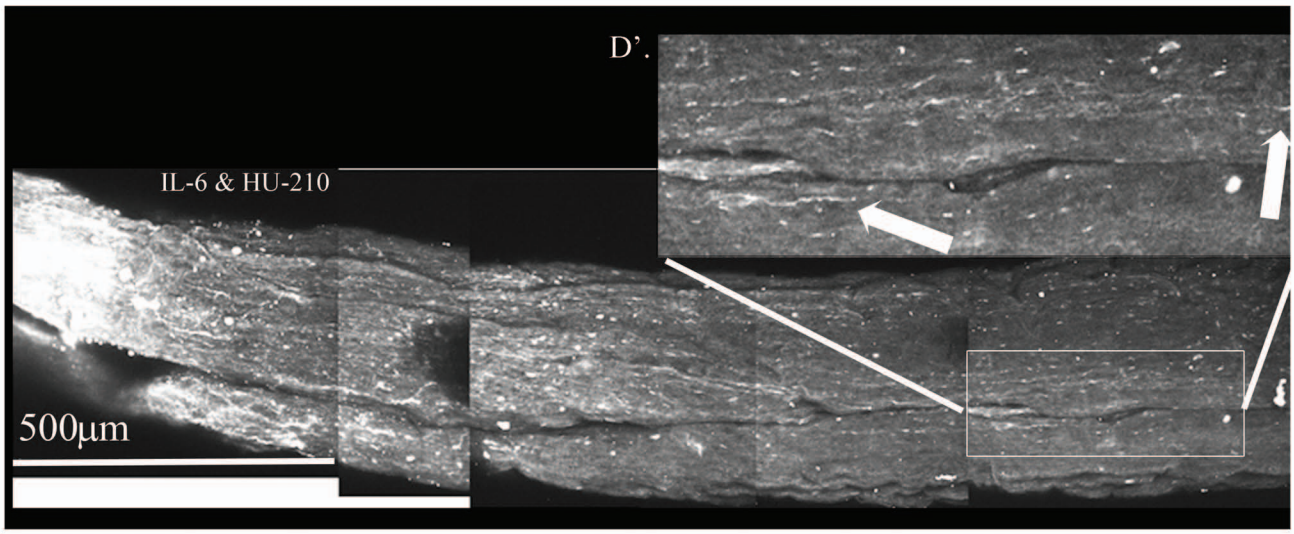

E.

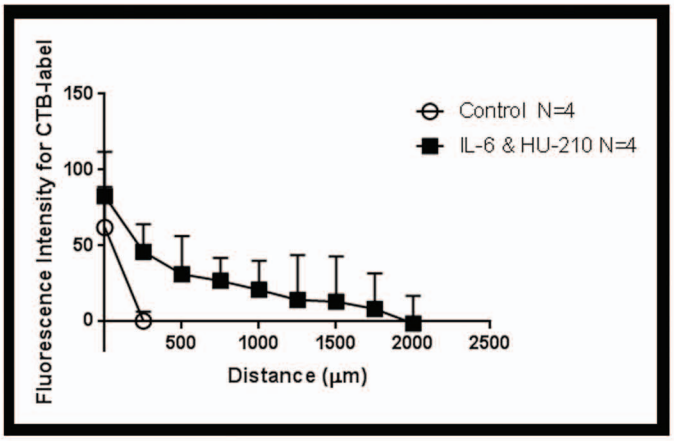

F.

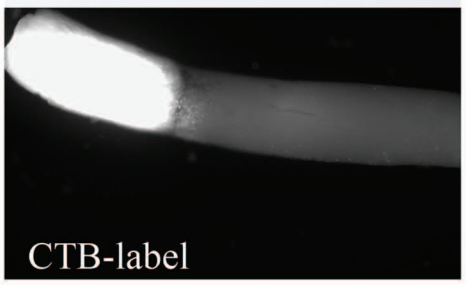

bioRxiv preprint doi: https://doi.org/10.1101/157099; this version posted September 21, 2018. The copyright holder for this preprint (which was not certified by peer review) is the author/funder, who has granted bioRxiv a license to display the preprint in perpetuity. It is made available under aCC-BY-NC-ND 4.0 International license.

Figure 3: Combination of IL-6 and HU-210 injected intravitreally promotes axonal regeneration in the crushed rat optic nerve (ONC) model. Fischer adult rats had unilateral ONC performed followed by intravitreal injections of either 0.5% DMSO for vehicle control (A) or the combination of IL-6 and HU-210 (B). After 2 weeks the nerves were removed, sectioned and immunolabeled with GAP-43. Controls had clear crush sites but no GAP-43 labeled axons crossing the crush site, while IL-6 and HU-210 had regenerating axons nearly 3 mm away as indicated by arrows. CTB-labeled regenerating axons within the whole nerve were detected after applying the 3-DISCO clearing technique. Control animals had clear crush sites with few fibers crossing (C). However, with IL-6 and HU-210 treatment we could detect CTB-labeled axons within the entire nerve bundle shown (D), above the boxed panel (D') is a magnified region demarcated by the white bars, showing the extent of regenerating axons over 2 mm away from the crush site, as pointed out by the white arrows. We quantified the extent of axonal regeneration in these chemically cleared nerves labeled with CTB using ImageJ analysis (E). Untreated crushed optic nerve was labeled with CTB immediately after injury and 3 days after crush we viewed the nerve under the light microscope (F, top image), and the CTB-label under fluorescence, showing no spared fibers (F, bottom image).

bioRxiv preprint doi: https://doi.org/10.1101/157099 this version posted September 20, 2017. The copyright holder for this preprint (which was not certified by peer review) is the author/funder, who has granted bioRxiv a license to display the preprint in perpetuity. It is made available under CC-BY-NC-ND 4.0 International license

Figure 4

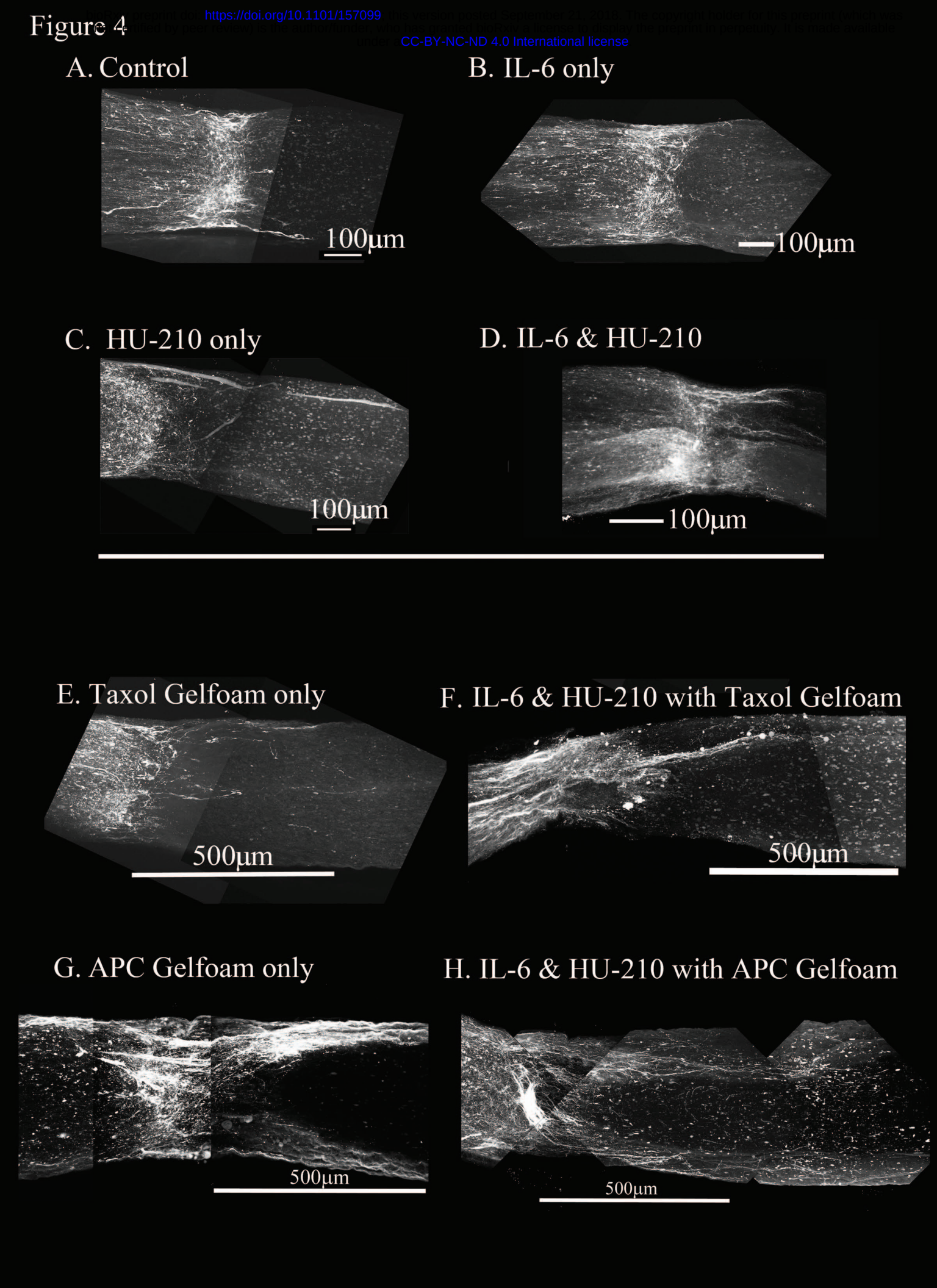

bioRxiv preprint doi: https://doi.org/10.1101/157099; this version posted September 21, 2018. The copyright holder for this preprint (which was not certified by peer review) is the author/funder, who has granted bioRxiv a license to display the preprint in perpetuity. It is made available under aCC-BY-NC-ND 4.0 International license.

Figure 4: ONC axonal regeneration in response to the drugs tested in Long Evans Rats.

Using the rat ONC model and retrogradely labeling regenerating axons with Cholera Toxin B (CTB) by intravitreal injections into the retina 3 days prior to sacrificing and then chemical clearing using the 3-DISCO technique, we were visualizing the whole nerve and not just sections using a Multiphoton microscope. Note these images are not to the scale, so they have individual scale bars. Control (A) not treated animals, have few labeled axons crossing a short distance (less than 0.2mm from the crush site), this was consistent for IL-6 (B) and HU-210 (C) tested individually as well, where no significant axonal regeneration was detected past the crush site. Combining intravitreal injections of IL-6 and HU-210 also promoted limited growth (D). Taxol applied in gelfoam alone had promoted limited axonal regeneration (E). Adding Taxol gelfoam with IL-6 and HU-210 injections resulted in more robust growth, but still less than 1mm from the crush site (F). APC gelfoam alone also promoted modest axonal regeneration from the crush site (G). Slightly more robust growth is detected when we combine IL-6 and HU-210 with APC gelfoam.

bioRxiv preprint doi: https://doi.org/10.1101/157099; this version posted September 21, 2018. The copyright holder for this preprint (which was not certified by peer review) is the author/funder, who has granted bioRxiv a license to display the preprint in perpetuity. It is made available under a CC-BY-NC-ND 4.0 International license.

Figure 5-1

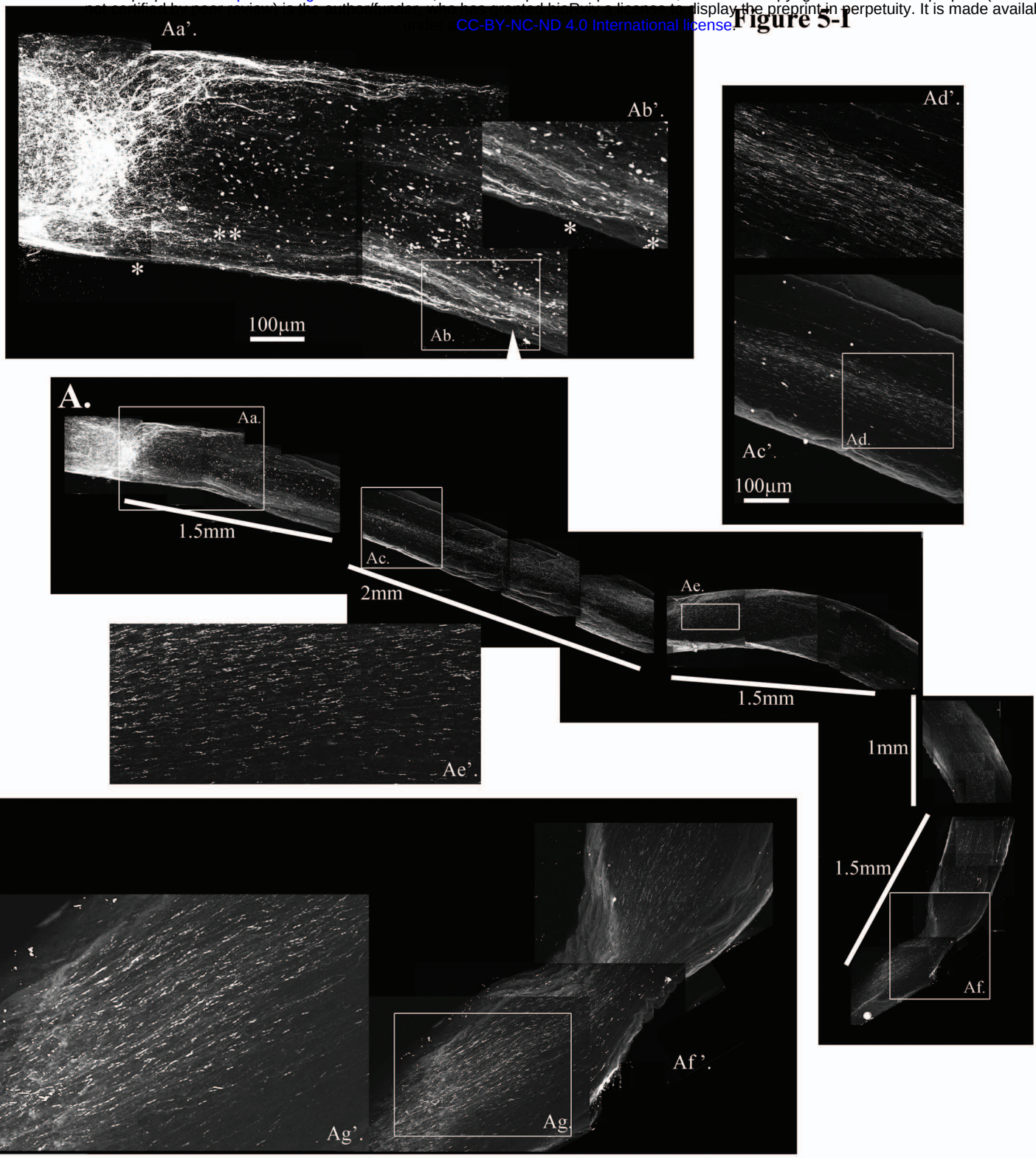

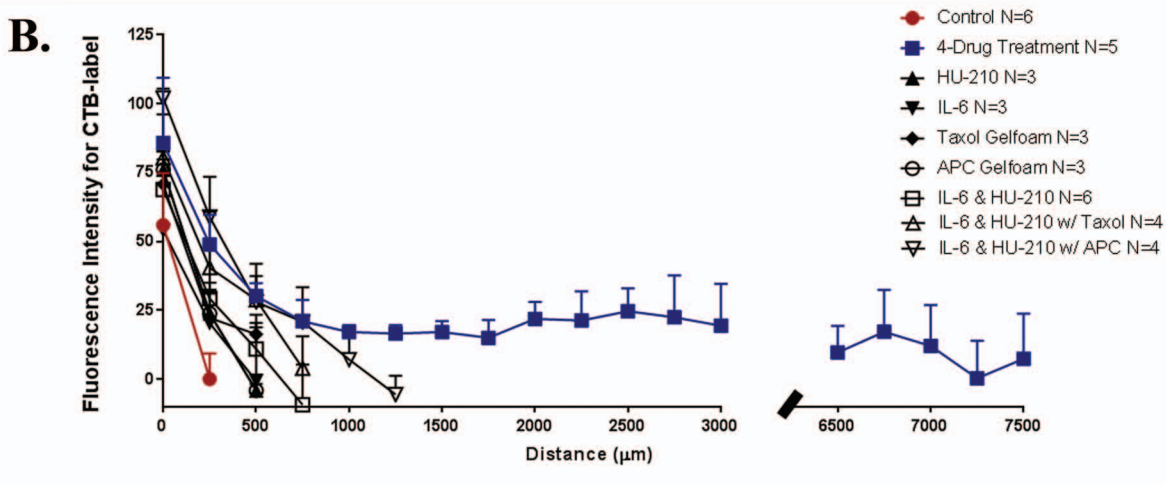

CC-BY-NC-ND 4.0 International license

Figure 5-II

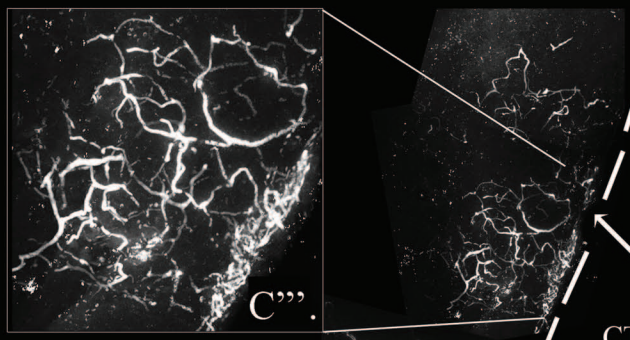

CTB-labeled Axons at outer border of Chiasm and brain

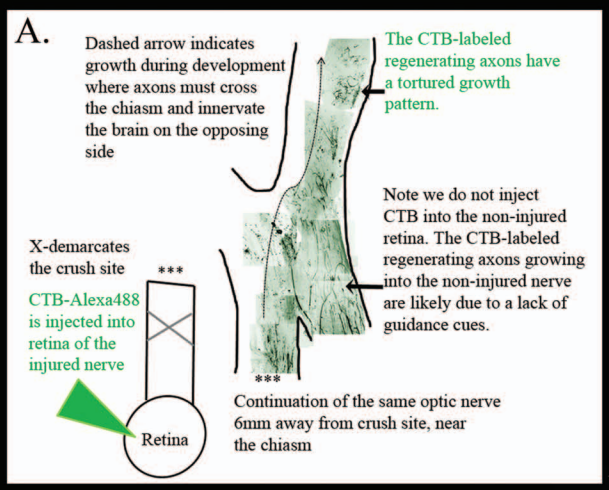

Torturous axon growth highlighted in blowups

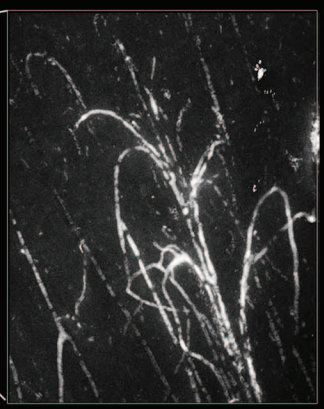

Crushed optic nerve CTB-labeled axons growing in direction of the arrow

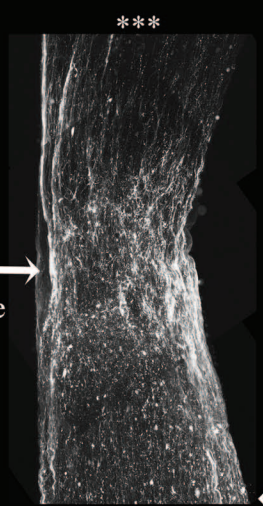

Uninjured nerve with CTB-labeled axons growing due to lack of guidance cues

C. *Chiasm*

***

From Retina injected with CTB

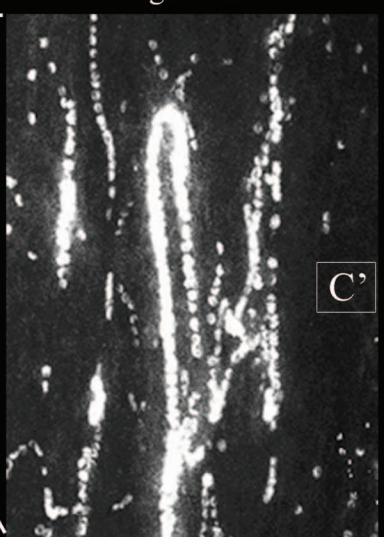

***Continuation of the same optic nerve 6mm away from the crush site near the chiasm

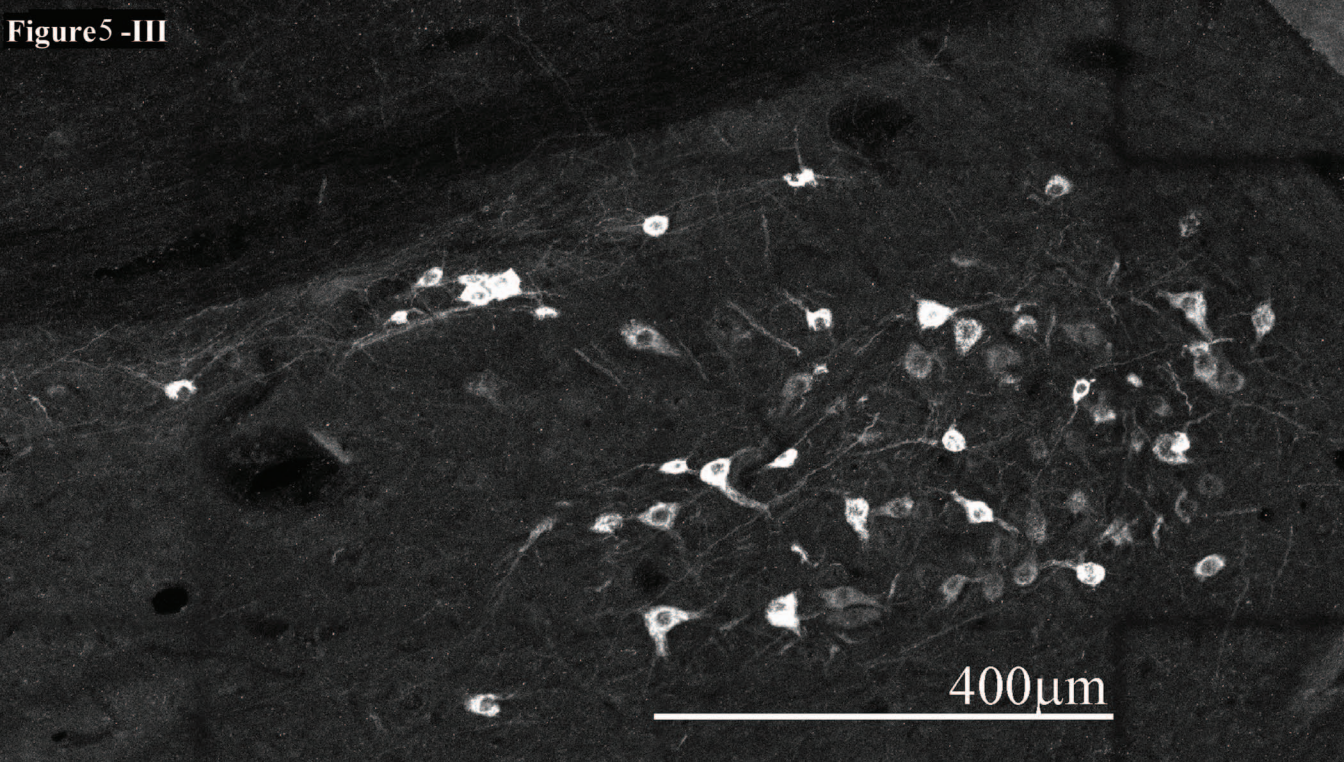
Figure5 -III
400μm

bioRxiv preprint doi: https://doi.org/10.1101/157099; this version posted September 21, 2018. The copyright holder for this preprint (which was not certified by peer review) is the author/funder, who has granted bioRxiv a license to display the preprint in perpetuity. It is made available under aCC-BY-NC-ND 4.0 International license.

Figure 5. four-Drug combination in the rat ONC model promotes axonal regeneration to the chiasm and the brain. 5-I: A. With 4-Drug treatment we see abundant a synergistic effect where our 4-drugs promoted growth of CTB-labeled fibers from the crush site (A and blow up of area in the white box in Aa'). This animal we waited 3 days post-CTB label to look at the axonal regeneration. In Ab with a white arrowhead and Ab' we point out the fibers growing along the edge with an asterisk (*) that end as indicated by the white arrow. Blow up of that area in the white box is in Ab', with * demarcating where fibers growing along the edge end. The double asterisk (**) in Aa' point out the axons protruding from the crush site. Ac. is a blowup of the area in the white box about 1.5mm from the crush site, CTB labeled fibers are observed in the blow up of the white box in Ac' and in higher magnification in Ad and Ad'. Ae. Blow up of the region about 3.5mm from the crush site showing punctate CTB labeled fibers in Ae'. The CTB label continues to the chiasm, as shown in the blow up of the chiasm in Af, with a further blow up in Af' nearly 7.5mm from the crush site, with a higher magnification view in Ag and Ag'. **B**. Graph measuring the longest CTB-labeled axon per treatment indicated using ImageJ analysis. A more detailed breakdown of the number of animals that regenerated axons are provided in Table 1. **5-II:** Second animal with 4-Drug treatment revealing growth to the chiasm and the brain, this animal we waited 7days post CTB-labeling. (A) Cartoon representation of the chiasm in the figure, details the CTB coupled to Alexa 488 is injected into the retina of the injured nerve. The arrow in the figure is the normal path of growth of majority of the axons in development. (B) The crush site of the nerve treated with four-Drug combination, *** indicates the nerve image is discontinuous and imaging of the CTB-label. (C) For the same nerve as indicated in B., the ***demarcates the chiasm. Several CTB-labeled axons are found growing into the uninjured nerve with a torturous growth pattern. Several blow-up images (C'-C''') highlight the torturous growth observed. (D) Brain sections that are immunostained for CTB revealed CTB labeled neurons in the superior colliculus. A blow-up of this section is on the following page (D'). **5-III:** A magnified view of the brain section in Fig 5-IID.

Figure 6

A.

Pattern Electroretinograms

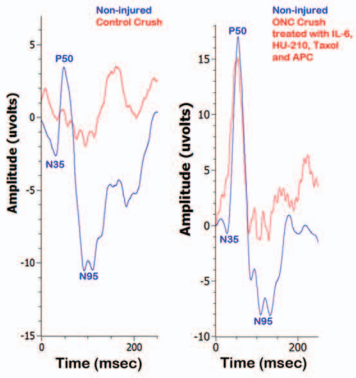

Flash ERG

B.

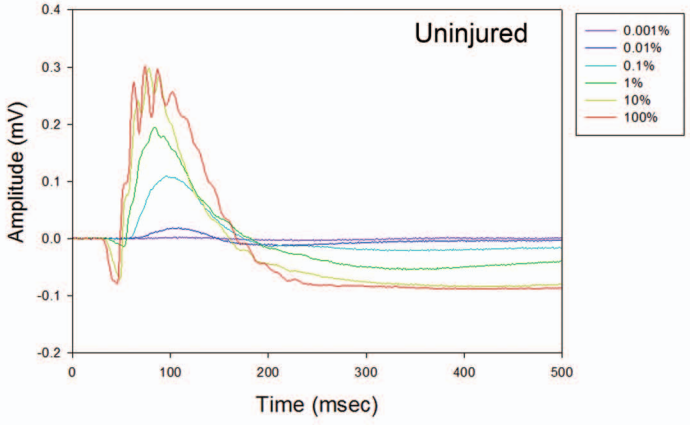

C.

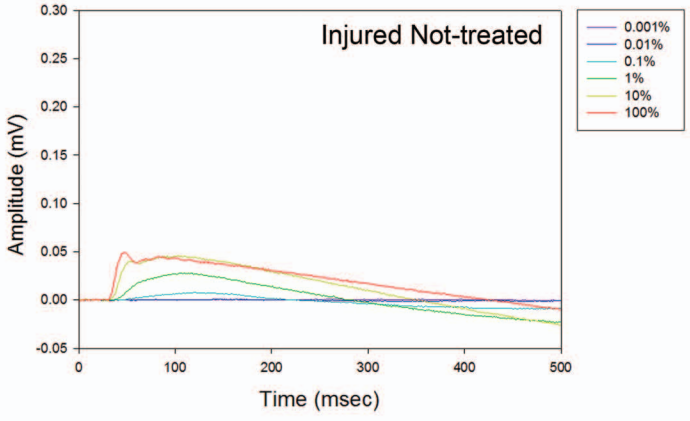

D.

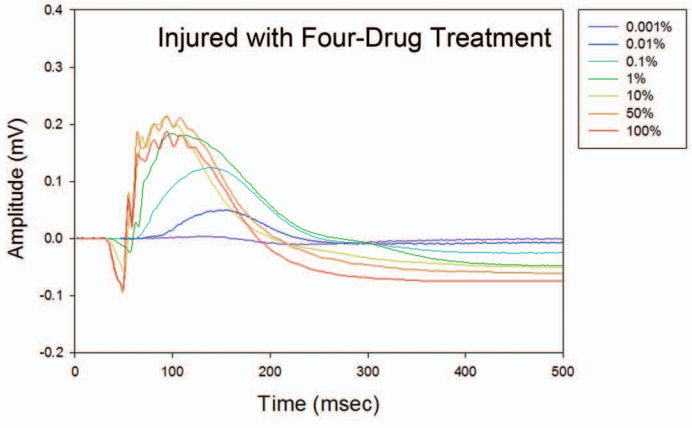

Visual Evoked Potential (VEP)

E.

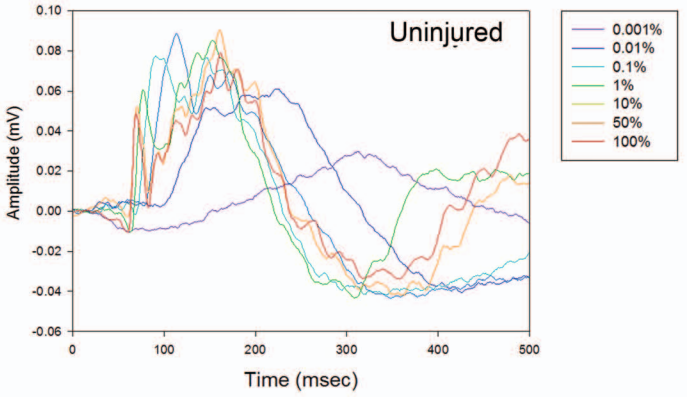

F.

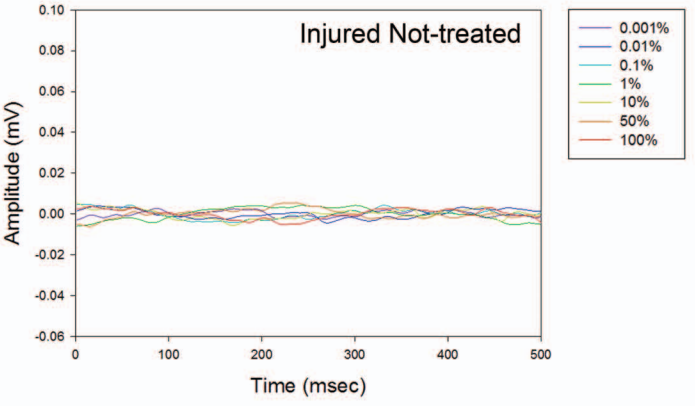

G.

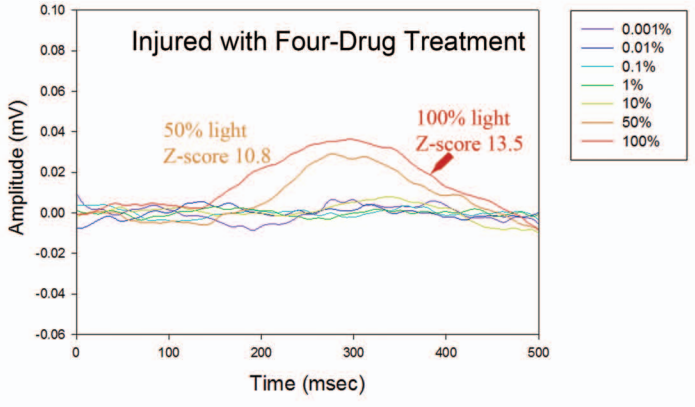

H.

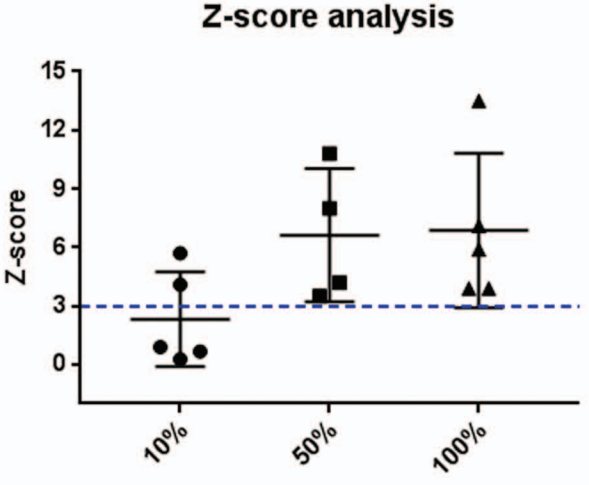

bioRxiv preprint doi: https://doi.org/10.1101/157099; this version posted September 21, 2018. The copyright holder for this preprint (which was not certified by peer review) is the author/funder, who has granted bioRxiv a license to display the preprint in perpetuity. It is made available under aCC-BY-NC-ND 4.0 International license.

Figure 6. The four-drug combination enhances pattern electroretinograms and VEP responses compared to injured optic nerve treated with vehicle only. (A) We performed pattern electroretinograms (pERG) using the UTAS system (LKC Technologies). Two weeks after optic nerve crushes anesthetized animals had contact lens electrodes to record ERGs in response to pattern stimuli, we recorded from both the non-injured (blue) and injured (red) with (right panel) or without (left panel) the four-drug combination treatment. In representative recordings of control animals with vehicle only (left panel) had aberrant pERGs compared to their non-injured eye, while animals with the four-drug combination had pERGs in their injured eye (right panel) approaching baseline levels of their non-injured eye. These are individual raw recordings and not normalized. We performed flash electroretinograms (fERG) which is a strong response to the natural stimuli of light in a graded series of intensities (0.001 to 100% max flash intensity). Representative panels of flash electroretinograms (fERG) traces in response to full light spectrum: B: Uninjured, C: Injured Not-treated, and D: Injured with 4-drug treatment. We simultaneously recorded visual evoked potentials (VEP, E-G) in the brain. Flashes were delivered under dark adapted conditions. Uninjured nerve recordings had graded VEP response to increasing intensity of light. In the uninjured eye (E) the VEP was slow for the dimmest flash, peaking around 300ms, and had fast onset with multiple wave components and compound action potentials for the brightest flashes. Injured eyes with no treatment (F) have no detectable VEP activity. The VEP in several treated animals (G) exhibited a slow waveform in the response to the highest intensities of light (50 and 100%), suggesting that some axons regenerated all the way to the brain. Z-score values for 50% and 100% are shown in the figure, indicating they are significantly different from the noise. (H) Summary of the Z-scores calculated for the 5 animals with four-drug treatment that showed VEP signals at some intensity. Of the 5 animals tested at 10%, 2/5 met the criterion to be above a Z-score of 3 (blue dashed line); all 4 tested at 50%, showed a response; and all 5 tested at 100% showed a response. The one animal not tested at 50% showed VEPs at 10% and 100%.